Cement and Concrete Research 40 (2010) 508–516

Contents lists available at ScienceDirect

Cement and Concrete Research

journal homepage: http://ees.elsevier.com/CEMCON/default.asp

Effects of aggregate size and alkali content on ASR expansion

Stéphane Multon [a], Martin Cyr [a,*], Alain Sellier [a], Paco Diederich [a], Laurent Petit [b]

[a] Université de Toulouse; UPS, INSA; LMDC (Laboratoire Matériaux et Durabilité des Constructions); 135, avenue de Rangueil; F-31 077 TOULOUSE cedex 4, France
[b] Electricité de France (EDF) – Recherche et Développement, Avenue des Renardières, 77818 MORET SUR LOING Cedex, France

ARTICLE INFO

Article history:
Received 24 October 2008
Accepted 3 August 2009

Keywords:
Particle size distribution (B)
Alkali-aggregate reaction (C)
Alkalis (D)
Modeling (E)
Pessimum of aggregate size

ABSTRACT

Attempts to model ASR expansion are usually limited by the difficulty of taking into account the heterogeneous nature and size range of reactive aggregates. This work is a part of an overall project aimed at developing models to predict the potential expansion of concrete containing alkali-reactive aggregates. The paper gives measurements in order to provide experimental data concerning the effect of particle size of an alkali-reactive siliceous limestone on mortar expansion. Results show that no expansion was measured on the mortars using small particles (under 80 µm) while the coarse particles (0.63–1.25 mm) gave the largest expansions (0.33%). When two sizes of aggregate were used, ASR-expansions decreased with the proportion of small particles. Models are proposed to study correlations between the measured expansions and parameters such as the size of aggregates and the alkali and reactive silica contents. The pessimum effect of reactive aggregate size is assessed and the consequences on accelerated laboratory tests are discussed.

1. Introduction

Reassessment of structures (bridges and dams) damaged by the Alkali-Silica-Reaction is of prime importance for engineering structure owners. The gel volume formed by the chemical reaction can be used as input data to structural models [1]. One of the main difficulties is to assess the volume of this gel [2]. Microscopic models [3–7] could be one method of doing this. Such models should be able to predict the differences of expansions with the variation of all influential parameters (size of aggregate, silica content, alkali content, etc.) and have to be compared with experimental results.

Numerous papers deal with the effect of particle size of reactive aggregates on the expansion due to ASR. Experiments have been performed on several types of aggregates. It seems that which aggregate size causes the highest ASR expansion depends on the nature and composition of the aggregate. Significant differences have been observed between rapid and slow alkali-reactive aggregates. Opal was one of the earliest and most widely used aggregates in laboratory studies of the size effect [8–12]. Investigations on the size effect have also been performed with different kinds of silica glass, fused silica, waste silica glass, andesite, siliceous limestone, quartzite, greywacke, chert, mylonite, flint and sandstone [13–18]. In spite of all these studies, it is difficult to generalize about the effect of the particle size of reactive aggregates, since conflicting results exist concerning the most damaging size that leads to the highest ASR expansion. All the results available in the literature were obtained using different experimental conditions and the effects due to coupling with other important parameters, such as Na/Si ratio, have been often neglected.

A few papers deal with the effect of size for reactive siliceous limestone [6,8,9,19]. This type of aggregate has been used in many damaged structures in France. Therefore, in order to test models to predict the potential expansion of concrete containing such alkali-reactive aggregates, tests have been performed to provide experimental data on the effect of particle size of an alkali-reactive siliceous limestone on mortar expansion. This paper presents the experimental results (expansion measurements performed over more than 500 days at 60 °C) and gives data necessary for model development.

Sixteen mix-designs were studied and special attention was paid to the proportions of alkalis (Na_2O_{eq}) in the mixtures and reactive silica in the aggregate. First, the paper presents the experimental conditions of the tests. Then, the measurements of ASR-expansions are presented in two parts: experiments on mortars containing one reactive size distribution (0–80 µm, 80–160 µm, 160–315 µm, 315–630 µm; 630–1250 µm, or 1250–2500 µm) and experiments on mortars containing mixes of two sizes of aggregate (0–80 µm and 1250–3150 µm) with increasing 0–80 µm reactive aggregate content. Finally, models are proposed to analyze the experimental results by studying correlations between the measured expansions and parameters such as the size of aggregates and the alkali and reactive silica contents. A time-dependent model allows the pessimum effect of reactive aggregate size to be assessed and its consequences on accelerated laboratory tests are discussed at the end.

* Corresponding author.
E-mail address: cyr@insa-toulouse.fr (M. Cyr).

0008-8846/$ – see front matter © 2009 Elsevier Ltd. All rights reserved.
doi:10.1016/j.cemconres.2009.08.002

2. Experimental conditions

2.1. Materials

The cement used was a standard CEM I 52,5R with a specific gravity of 3.1 and a specific surface area (Blaine) of 400 m^2/kg. Its chemical composition is given in Table 1. The aggregates were crushed sands (jaw crusher): a non-reactive marble (NR) and a reactive siliceous limestone (R). The chemical composition of aggregates NR and R are given in Table 1. The non-reactive marble was mainly composed of calcite. The reactive siliceous limestone contained mostly calcite and quartz, with traces of dolomite, feldspars and phyllosilicates. In order to control the particle size distribution of the aggregates in the mortars, the aggregate samples were divided into several particle size fractions: 0–80, 80–160, 160–315, 315–630, 630–1250, 1250–2500 and 1250–3150 μm). Details of the aggregate combinations are given in Section 2.3.

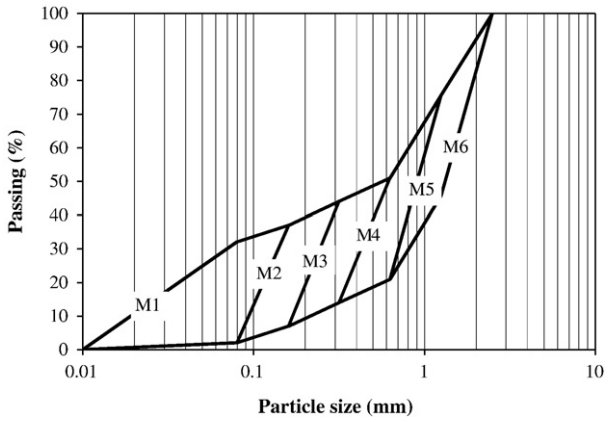

Fig. 1. Particle size distributions of mortars M1 to M6.

2.2. Methods

Expansion was measured on mortar prisms (2 × 2 × 16 cm) with a sand (1512 kg/m^3) to cement (504 kg/m^3) ratio of 3. The mortar prisms were demolded 24 h after casting and were then kept in sealed bags at 20 °C until 28 days. At 28 days of age, the prisms were stored at 60 °C, after being placed on grids in watertight containers containing 20 mm of water (mortar bars were not in contact with water). Salt (K_2SO_4) was added to the water (above saturation) in order to maintain a relative humidity above 95% in the containers and to try to avoid condensation on the specimens. Expansion was measured using the scale micrometer method (specimens had shrinkage bolts at both ends). Each measurement was the mean of three values from three replicate specimens. Expansion measurements were performed after the containers and the prisms had been cooled for 24 h at 20 °C.

In order to reach specific Na/Si ratios, mixtures were adjusted to alkali contents (Na_2O_{eq}) of 6.2, 8.1 and 9.9 kg of alkali per m^3 of mortar by adding NaOH in the mixing water. An alkali-free superplasticizer was used (0.5% dry matter of cement mass) in mortars to achieve a proper set in the molds.

For the first part, the water–cement ratio was 0.5. For the second part, the largest content (40%) of fine reactive particles (0–80 μm) absorbed too much water during the casting, the mortar was too dry to be cast with a ratio of 0.5 (even with a superplasticizer). Therefore, the water–cement ratio was increased to 0.6.

2.3. Experimental program

2.3.1. Size effect

The first experimentation presented in this paper concerns the study of size effects of the reactive siliceous limestone on ASR expansions. In this part, six particle size fractions were studied in mortars: 0–80 (mortar M1), 80–160 (M2), 160–315 (M3), 315–630 (M4), 630–1250 (M5) and 1250–2500 μm (M6). These mortars contained 8.1 kg of alkali per m^3 of mortar. In order to obtain significant expansions with the aggregate studied in this paper, the content of reactive aggregate had to be at least 30%. The particle size distributions (Fig. 1) were obtained by adding 30% of reactive aggregate of the six different fractions to 70% of a continuous size distribution (0–2500 mm) of non-reactive aggregate. Therefore, the particle size distributions were different for the six mortars. The effect of such differences in particle size distribution on the porosity of mortars was studied on mortars containing only non-reactive particles. Porosities measured using the AFPC-AFREM method [20] laid between 17.3 and 18.2%. The differences did not appear to be significant compared to difference of 1% which could be obtained during measurements made on three specimens of a given mortar.

2.3.2. Effect of fine reactive aggregate

For the second part of the experimentation, reactive particles of two sizes were used: 0–80 μm and 1250–3150 μm, in mortars containing 6.2 and 9.9 kg of alkalis per m^3 of mortar. Aggregates in all mortars had an equivalent particle size distribution and were composed of 40% of 0–80 μm particles, 30% of 315–630 μm particles and 30% of 1250–3150 μm particles. For the five reactive mortar mixtures studied, all the 315–630 μm particles were non-reactive and all the 1250–3150 μm particles were reactive. Only the nature of 0–80 μm particles changed: mortars M7, M8, M9, M10 and M11 contained 0%, 10%, 20%, 30% and 40% of 0–80 μm reactive aggregate and 40%, 30%, 20%, 10% and 0% of 0–80 μm non-reactive aggregate, respectively. Therefore, mortars M7, M8, M9, M10 and M11 contained a total of 30%, 40%, 50%, 60% and 70% of reactive particles, respectively. Moreover, measurements were performed on two reference mortars with only non-reactive aggregates (one for each alkali content).

3. Experimental results

3.1. Size effect

The experimental results are presented in Figs. 2 and 3. The ASR-expansions presented in these figures were obtained by subtracting the expansion of the reference mortar (without reactive aggregate) from the total expansion, as already proposed by some authors [21–23]. The long-term expansion of the reference mortars was 0.03%. The kinetics of the ASR-expansions measured for 500 days are given in Fig. 2. After 500 days of exposure at 60 °C and 95% R.H., mortars containing small reactive particles (0–80 and 80–160 μm) showed ASR-expansions lower than about 0.01% (Fig. 3). ASR-expansions

Table 1
Chemical composition of cement and aggregates (% by mass).

	SiO_2	Al_2O_3	Fe_2O_3	CaO	MgO	Na_2O	K_2O	Na_2O_{eq}	SO_3	LOI
Cement	20.1	5.6	2.0	62.5	3.1	0.2	0.9	0.8	3.2	1.7
Non-reactive marble	–	–	–	54.4	0.5	0.001	–	–	0.01	43.0
Reactive siliceous limestone (1.25–3.15 mm)	20.0	1.3	0.6	40.6	1.2	0.4	0.4	0.7	0.3	34.7

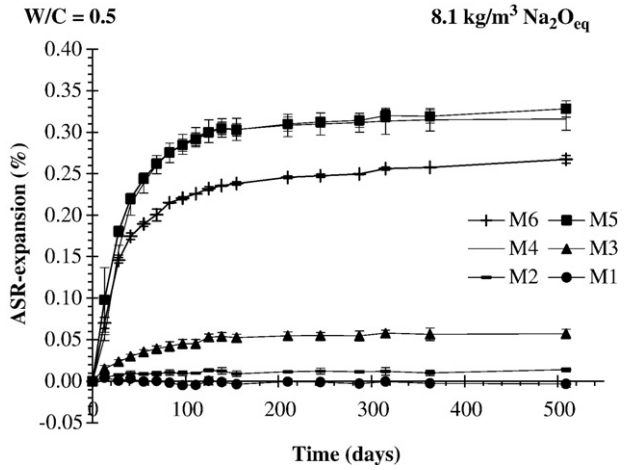

Fig. 2. ASR-expansions of mortars containing 30% of reactive particles of size 0–80 (M1), 80–160 (M2), 160–315 (M3), 315–630 (M4), 630–1250 (M5), 1250–2500 µm (M6) and 70% of continuous 0–2500 µm non-reactive sand.

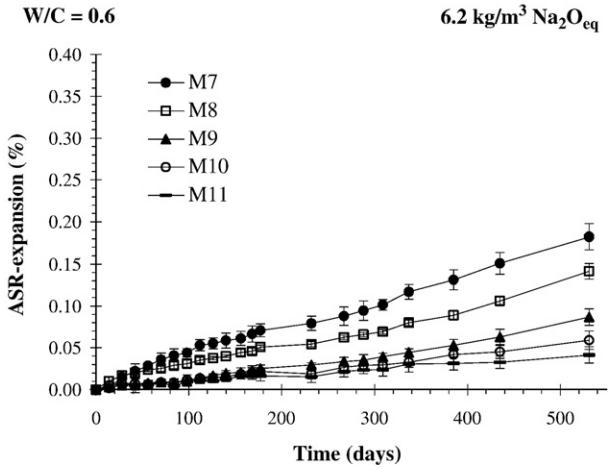

Fig. 4. ASR-expansions of mortars containing variable proportions of reactive aggregates (mix of reactive particles of two sizes: 0–80 µm and 1250–3150 µm) for 6.2 kg of alkalis per kg of mortar.

were measured for all the other mortars using particles larger than 160 µm: 0.057% for 160–315 µm reactive particles, 0.315% for 315–630 µm particles, 0.328% for 630–1250 µm particles and 0.267% for 1250–2500 µm particles.

3.2. Effect of fine reactive aggregate

Measurements of the ASR-expansions were taken for more than 500 days for the two alkali contents (Figs. 4 and 5). The ASR-expansions presented were obtained by subtracting the expansion of the reference mortar from the total expansion. The long-term expansions of the reference mortars were 0.02% and 0.03% for the low and the high alkali contents, respectively. For the two alkali contents, the mortars containing only the large reactive particles (M7) showed the largest ASR-expansions. Fig. 6 shows the last ASR-expansion measured, related to the amount of fine reactive particles in the mortar mixtures. ASR-expansion decreased with the amount of fine reactive particles in the mortars: the more fine reactive particles the mortar contained, the smaller was the ASR-expansion.

4. Model and discussion

The models presented in this section aim to improve the understanding of the experimental results obtained in the first part. The first model assesses the asymptotic expansion of mortars containing only one size (first set of experiments) or the mixture of two sizes (second set of experiments) of reactive aggregates. In order to integrate the dependence of swelling over time, a second model is then proposed. It will be shown that for a given duration of test and a given alkali content, the expansion is maximized for a specific range of aggregate size (pessimum effect). However, the time-dependent model does not consider the mixture of aggregates of different sizes for the moment. Finally, it should be noted that the fitted parameters supplied here are only applicable for the aggregate studied in this paper.

4.1. Asymptotic expansion model

4.1.1. Effects of aggregate size and alkali content on asymptotic expansion

For this reactive limestone, no ASR expansion was measured for small reactive particles (less than 160 µm). ASR-expansion appeared for particles having diameters greater than 160 µm (Fig. 3). However, for the same content of reactive particles, the expansion was smaller for the 160–315 µm reactive particles than for the 315–630 µm reactive ones. The critical particle size that caused ASR-expansions was around 200 and 300 µm. ASR-expansions increased with the size of reactive particles between 0 and 630 µm. The ASR-expansion was very similar for the 315–630 µm particles and for the 630–1250 µm

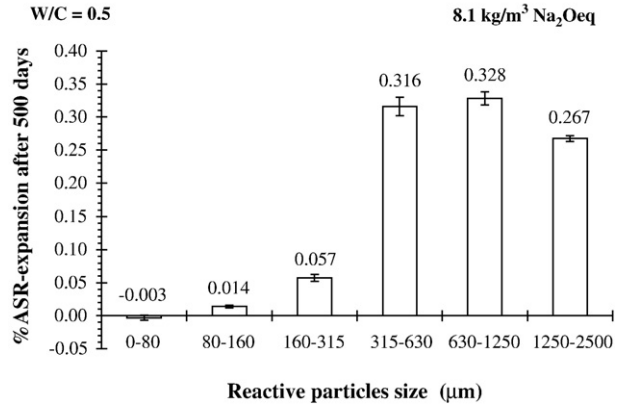

Fig. 3. ASR-expansions of mortars containing 30% of reactive particles of size 0–80 (M1), 80–160 (M2), 160–315 (M3), 315–630 (M4), 630–1250 (M5), 1250–2500 µm (M6) and 70% of continuous 0–2500 µm non-reactive sand after 500 days at 60 °C and 95% RH.

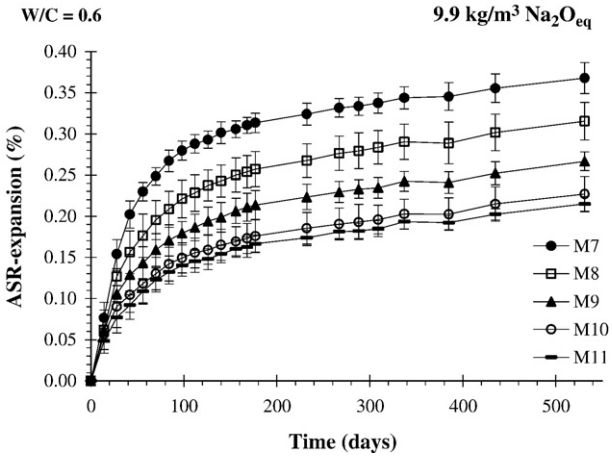

Fig. 5. ASR-expansions of mortars containing various reactive aggregate contents (mix of reactive particles of two sizes: 0–80 µm and 1250–3150 µm) for 9.9 kg of alkalis per kg of mortar.

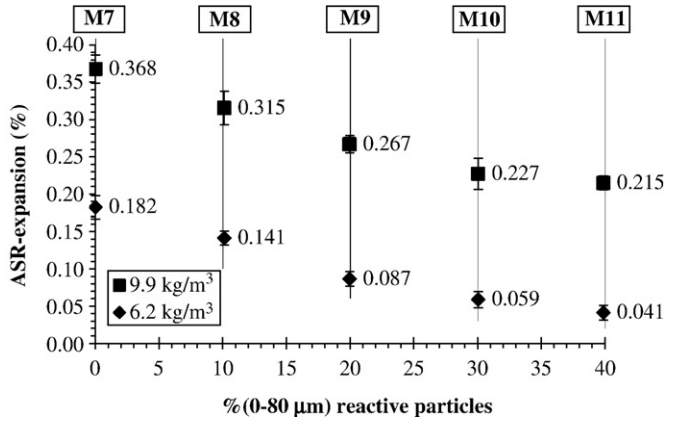

Fig. 6. ASR-expansions at 500 days of mortars containing various reactive aggregates contents (mix of reactive particles of two sizes: 0–80 µm and 1250–3150 µm) for 6.2 and 9.9 kg of alkalis per kg of mortar. Effect of the amount of fine (0–80 µm) reactive particles.

ones. Finally, the larger reactive particles showed lower expansions (Fig. 3). This pessimum effect, which has already been observed for other reactive aggregates [10,13], is assessed in the last part of this paper.

The expansion of the mortar is caused by the expansions of the ASR-gels. It can be assumed that this expansion is caused by the volume variation of the aggregate (in presence of gel). For the sake of simplicity, it is assumed in this paper that the mortar expansion due to ASR (ε_{ASR}) is proportional to the aggregate expansion (Eq. (1)). For several sizes of reactive particles, the aggregate expansion is the sum of the expansions of all the reactive aggregates.

$$\varepsilon_{ASR} = k \cdot \sum_{i=1}^{N_{rc}} \varphi_i^{agg} \varepsilon_i^{agg} \tag{1}$$

where ε_i^{agg} is the expansion of one reactive aggregate of class i, φ_i^{agg} is the volume fraction of reactive aggregates of class i relative to the mortar volume (total volume of reactive aggregate of class i/total volume of the mortar), N_{rc} is the number of classes of reactive aggregates and k is the fraction of expansion due to ASR related to the expansion of reactive aggregates.

The mortar expansion is assumed to be due to the aggregate expansion. If $k=1$, the mortar expansion is equal to the aggregate expansion (weighted by the volume fraction of reactive aggregates in the mortar). In reality, k has to be equal to or lower than 1, since the mortar expands less than the aggregate due to the mechanical effect of cement paste. The decrease of the value of the parameter k corresponds to the increase of the restraint of the cement paste on the aggregate. During ASR, when the aggregate swells, the cement paste is subjected to tensile stresses. Therefore, the effect of restraint is limited and the parameter k should not be too small.

During the formation of the ASR-gel, a part of the gel can migrate through the porosity close to the aggregate without causing expansion. Therefore, the aggregate expansion for one aggregate i can be described by Eq. (2).

$$\varepsilon_i^{agg} = \frac{\langle V_i^{gel} - V_i^{poro} \rangle^+}{V_i^{agg}} \tag{2}$$

With:

- V_i^{agg}: the volume of one reactive particle, $V_i^{agg} = \frac{4}{3}\pi \cdot R_i^3$, where R_i is the radius of the reactive particle.
- $(X)^+$: the positive part of X: if $X<0$, $(X)^+=0$ otherwise $(X)^+=X$
- V_i^{poro}: the volume of the porosity close to the reactive aggregate in which the ASR gel can migrate without causing expansion.

Assuming that the gel can migrate along the same distance of the aggregate l_c whatever the size of the aggregate (simplifying hypothesis), the volume of the porosity is given by Eq. (3), where φ^{void_mortar} is the porosity of the mortar.

$$V_i^{poro} = \frac{4}{3}\pi \cdot \left((R_i + l_c)^3 - R_i^3 \right) \cdot \varphi^{void\_mortar} \tag{3}$$

- V_i^{gel}: the volume of ASR gel formed in only one reactive particle.

The volume of gel V_i^{gel} is considered as proportional to the alkali content and the reactive aggregate volume, as defined by Eq. (4).

$$V_i^{gel} = \varphi_i^{gel} \cdot V_i^{agg} \tag{4}$$

where φ_i^{gel} is the volume fraction of gel related to the particles of class i. φ_i^{gel} can be seen as the volume of gel (m^3) per m^3 of aggregate: the higher the aggregate content, the higher the amount of gel. It also implies that for high alkali content, more silica is attacked.

According to previous results [31] which showed that it was reasonable to use linear relationships to express the expansions of mortars versus the alkali content and versus the quantity of reactive particles, it can thus be assumed that φ_i^{gel} is proportional to:

- the alkali content of the mortar (AC) minus a threshold of alkalis (AC_{th}) under which no expansion occurs. Usually, high alkali content implies deeper aggregate attack, and thus a larger volume of gel per m^3 of reactive aggregate. However, many papers [24–30] have shown that, for low alkali contents (under a threshold lying between 3 and 5 kg/m^3), no expansion occurs. The value of AC_{th} used in this work was 3.5 kg/m^3 [31]. φ_{ref}^{gel} is a reference volume fraction of gel fitted from tests on mortars containing AC_{ref} (alkali content of the mortar in the first set of experiments — 8.1 kg/m^3). It was considered that there was no competition between the particles of different sizes.
- the volume fraction of the quantity of reactive particles of size i and the quantity of reactive aggregate in the mortar (expressed as volume fractions φ_i^{agg} and φ_{tot}^{gel}). In fact, the volume of gel created by the reactive particles of one size depends on the content of the reactive aggregates of this size compared to the content of all the reactive aggregates of the mortar. If there are only large particles, all alkalis can react with these particles but when small particles are added (as in the second set of experiments), the alkali content which reacts with the large particles has to decrease. It can be assessed by Eq. (5) for a time corresponding to the end of the tests.

From the above, the expression of the volume fraction of gel φ_i^{gel} can be given by Eq. (5).

$$\varphi_i^{gel} = \varphi_{ref}^{gel} \frac{\langle AC - AC_{th} \rangle^+}{\langle AC_{ref} - AC_{th} \rangle^+} \frac{\varphi_i^{agg}}{\varphi_{tot}^{agg}} \tag{5}$$

With:

- φ_{ref}^{gel}: reference volume fraction of gel fitted from tests with AC_{ref}
- φ_i^{agg}: volume fraction of reactive aggregates of class i relative to the mortar
- φ_{tot}^{agg}: volume fraction of reactive aggregates (total: all classes) relative to the mortar
- AC: alkali content of the mortar
- AC_{th}: value of the threshold in alkali (taken equal to 3.5 kg/m^3),
- AC_{ref}: alkali content of the mortar used to fit φ_{ref}^{gel} (8.1 kg/m^3),

The combination of Eqs. (1)–(5) for only one class of reactive particles (first set of experiments) leads to the Eq. (6).

$$\varepsilon_{ASR} = k \cdot \varphi_i^{agg} \cdot \left[\left\langle \varphi_i^{gel} - \varphi^{void\_mortar} \cdot \left(\frac{(R_i + l_c)^3}{R_i^3} - 1 \right) \right\rangle^+ \right] \quad (6)$$

With $\varphi_i^{gel} = \varphi_{ref}^{gel}$ since, for the first set of experiments, $AC = AC_{ref} = 8.1$ kg/m^3 and $\varphi_i^{agg} = \varphi_{tot}^{agg}$ (only one class of reactive particles).

In order to carry out this calculation, three parameters must be determined: l_c, φ_{ref}^{gel} and k. In this paper, several values for k between 0.1 and 1 are considered (for $k = 0.1$, the aggregate swells 10 times more than the mortars), and l_c and φ_{ref}^{gel} are calculated to minimize the deviation between the calculated value ε_{ASR} and the measured one. The value calculated using Eq. (5) (which is a volumetric deformation) was divided by 3 in order to obtain linear expansion (comparable to measured expansion on mortars).

The results of the calculations of the parameters are given in Table 2 and the calculated expansions are plotted in Fig. 7. Whatever the values of k, all the curves are quite similar, so only one curve is plotted (named 'Asymptotic expansion model'). For the lower values of k, the values of l_c and φ_{ref}^{gel} are maximal (Table 2). The larger the cement paste restraint is, the larger the volume of ASR-gel must be to obtain significant expansion; and if there is a lot of gel, l_c has to be large to prevent expansion for the small reactive particles. For the values of the parameter k higher than 0.1, the value of the parameter l_c ranges between 11 and 91 μm. Although the cement paste largely restrains the aggregate, this calculation can explain the increase of expansion with the size of the reactive particles.

To sum up, the model developed in this section assumes that the increase of ASR-expansion with the size of reactive particles can be explained by the effect of the porosity connected to the reactive aggregate. A porous crown of thickness l_c around the reactive aggregate, which is connected to the gel formation site, is defined. The volume of porosity to be filled around each particle of radius R_i before the expansion starts is given by Eq. (3). Fig. 8 shows the total volume of porosity to be filled ($V_i^{poro} \cdot N_i$, in m^3 per m^3 of mortar) when considering the number of reactive aggregate of each size (N_i). On the other hand, the volume of gel was computed according to Eqs. (4) and (5), for which the volume of gel was considered as proportional to the alkali content and the aggregate volume. The expansion of an unconstrained mortar prism was then taken as the volumetric change of the aggregate due to the gel volume not contained in the porous crown (Eqs. (1) and (2)). This simple relation allows the final expansion to be plotted against the aggregate radius R_i and the alkali content.

The calculation can be generalized for different sizes of reactive aggregates and different alkali contents. Fig. 9 shows the expansion of mortar prisms for ($20 < R < 1000$ μm) and ($3 < AC < 10$ kg/m^3). It can be seen that expansion increases linearly with the alkali content and non-linearly with the aggregate diameter. It could be concluded, abusively, from this figure that large aggregates and large alkali contents should lead to the highest expansion amplitude. However, even if a large aggregate presents a large expansion in this graph, a long test duration is needed in reality to obtain the final expansion amplitude, due to the long diffusion time for alkalis to reach the center of the particle (the porosity of this aggregate is less than 1%). In contrast, for small aggregates, alkali ingress is faster and the reaction occurs rapidly, but the porous crown delays the expansion.

Table 2
Model parameters.

k	0.1	0.25	0.5	0.75	1
l_c (μm)	91	41	22	15	11
φ_{ref}^{gel}	0.651	0.263	0.132	0.088	0.066

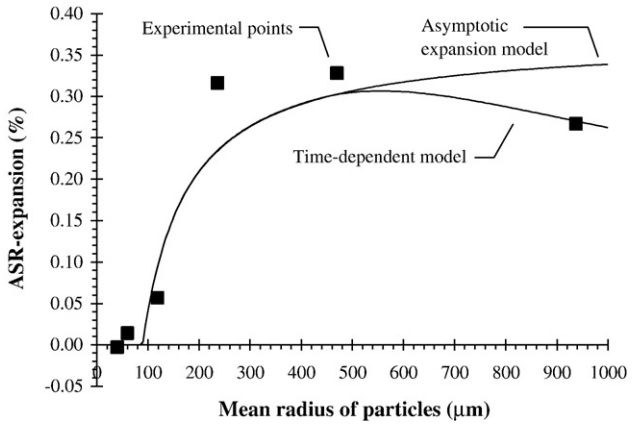

Fig. 7. ASR-expansion of mortars containing one size of reactive particles (M1 to M6) versus mean reactive particle size: comparison between experiments, asymptotic expansion model (Section 4.1) and time-dependent model (Section 4.2) (data: k, l_c and φ_{ref}^{gel} = any column of Table 2, $\varphi^{void\_mortar} = 0.17$, $AC_0 = 8.1$ kg/m^3, $AC_{th} = 3.5$ kg/m^3).

A pessimum size should exist for which the expansion is maximum for a given duration of test. This pessimum is obtained when the size of the aggregate is large enough to fill the connected porosity and the aggregate is completely attacked by the alkalis (while the larger sizes are not). In order to gain a better understanding of these phenomena, a time-dependent expansion model is proposed in Section 4.2.

4.1.2. Effect of fine reactive aggregate on asymptotic expansion

For mortars containing two sizes of reactive particles, the larger the content of reactive aggregate was, the smaller were the ASR-expansions (Fig. 6). In fact, the increase of the proportion of reactive aggregate was due to the increase of the smallest reactive particles (0–80 μm), while the proportion of the largest reactive particles (1250–3150 μm) was the same. The previous part showed that the smallest reactive particles did not cause expansion, but the largest ones expanded greatly. As the content of large particles was the same for all the five mortars (for one alkali content), expansions could be expected to be similar. However, the experimentation showed that the expansion decreased with increasing content of the small reactive particles. This effect has already been shown on concrete [32] and can sometimes be explained by the consumption of the alkalis by the small reactive particles. When aggregate powders are dispersed in a cement paste they release silica, resulting in a lowering of the Ca/Si ratio in C–S–H. It has been established that the ability of these low Ca/Si C–S–H to fix alkalis is enhanced. The depletion of free alkalis lowers the pH of the pore solution and, consequently, reduces the attack of

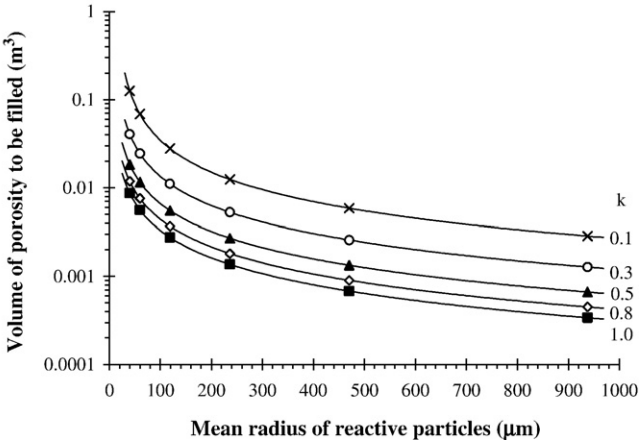

Fig. 8. Volume of porosity to be filled ($V_i^{poro} \cdot N_i$, in m^3 per m^3 of mortar on a logarithmic scale) when considering the number of reactive aggregate of each size (N_i).

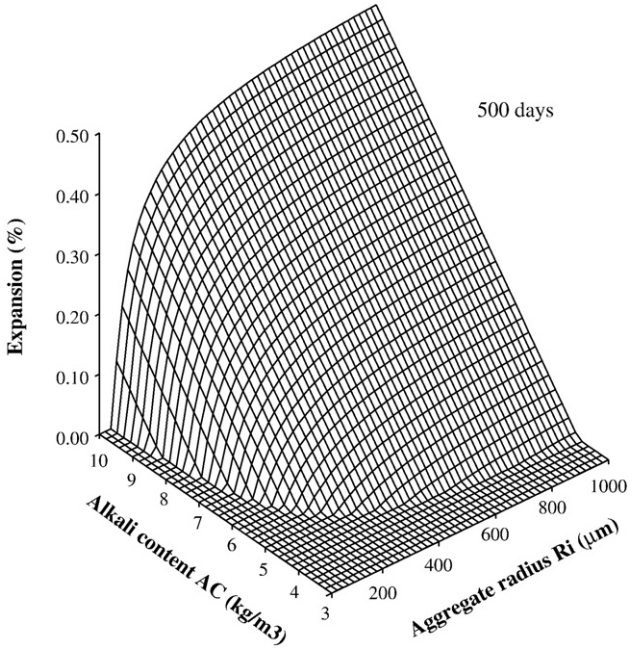

Fig. 9. Long-term expansion ($t = 500$ days) versus aggregate radius (R) and initial alkali content (AC) in mortars, calculated using the asymptotic expansion model (data: $k = 1$, $l_c = 11$ µm, $\varphi_{ref}^{gel} = 0.066$, $\varphi^{void\_mortar} = 0.17$, $AC_0 = 8.1$ kg/m^3, $AC_{th} = 3.5$ kg/m^3).

reactive aggregates. Finally the expansion is reduced or suppressed. However, it should be noted that this explanation is not satisfactory in all cases: some alkali-releasing mineral admixtures can inhibit the reaction, or sometimes only retard it (e.g. high alkali fly ashes).

Calculations were performed using Eqs. (1)–(5) for the two alkali contents and the two size classes of the second set of experiments, without any supplementary fitting. Fig. 10 gives the measured expansions versus the expansions assessed with the model with the parameters determined for $k = 1$ in the previous part (Table 2). As shown in Fig. 10, the model gives values not too far from the measured expansions. The mean deviation between calculated and measured expansions is about 18%. It can be partly explained by the deviation between the model and the measurements for the largest particle for the parameter determined in the previous part. The value calculated

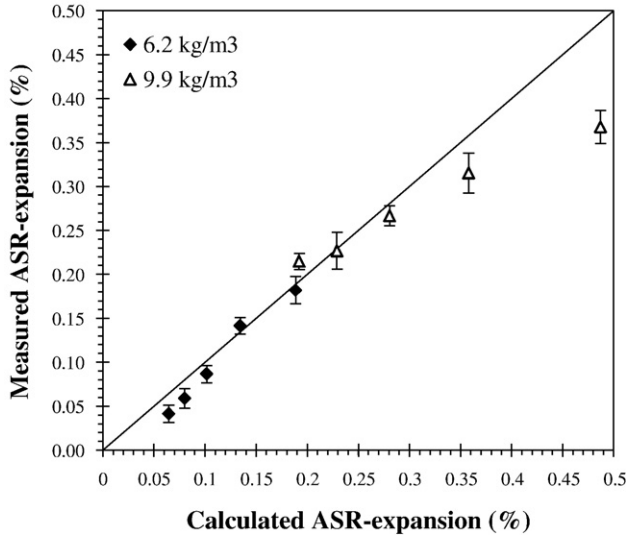

Fig. 10. Comparison between the expansions calculated using the asymptotic expansion model and the measured expansions, for mortars containing two sizes of reactive particles.

for the largest particle was about 30% higher than the measurement (Fig. 7). The overestimation of the expansion of coarse particles thus leads to an overestimate of the expansions of mortars containing mixtures of fine and coarse aggregates.

The model uses only proportionality between the parameters of volume of gel, alkali content and reactive aggregate content. It appears to be efficient for assessing ASR-expansions in this case for which mix designs and environmental conditions are perfectly known.

4.2. Time-dependent expansion model

In order to improve the model, it is decided to use a time-dependent model which allows us to take into account and explain the pessimum effect of coarse aggregates. A simplified diffusion model is chosen, which does not consider the mixture of aggregates of different sizes.

The simplest way to introduce the time effect in the previous model is to model the alkali ingress kinetics through a simple phenomenological function. For experimental and physical reasons, a square root function of the time is proposed [3]. The thickness of alkali penetration from the paste to the center of the aggregate is thus given by Eq. (7).

$$x(t) = R_{ref}\sqrt{\frac{t}{t_{ref}}} \tag{7}$$

With:

- $x(t)$: thickness of alkali penetration at a time t, from the paste to the center of the aggregate
- R_{ref}: radius of the aggregate used in the mortar for which the reference time t_{ref} is fitted
- t_{ref}: time necessary for alkali to reach the center of the aggregate of radius R_{ref}; fitted on experimental results such as $x(t_{ref}) = R_{ref}$. In our case, t_{ref} was fitted using the radius $R_{ref} = 236$ µm (mortar M4 – size of aggregate: 315–630 µm). It was assumed that the time necessary for alkali to reach the center of the aggregate of radius $R_{ref} = 236$ µm was 170 days (beginning of the asymptotic swelling of mortar M4, as seen on Fig. 2).
- t: duration of test

For a given duration t, the volume fraction of an aggregate of radius R_i affected by the reaction is then given by Eq. (8).

$$f(t) = \varphi_i^{asr\_agg}(t) = \frac{R_i^3 - \left(\langle R_i - x(t)\rangle^+\right)^3}{R_i^3} \tag{8}$$

The combination of Eqs. (1)–(5) and (7), (8) for only one class of reactive particles leads to the time-dependent model given by Eq. (9).

$$\begin{aligned}\varepsilon_{ASR}(t) &= k\cdot\varphi_i^{agg}\cdot\varepsilon_i^{agg}(t)\\ &= k\cdot\varphi_i^{agg}\cdot\frac{\langle V_i^{gel}\cdot f(t) - V_i^{poro}\rangle^+}{V_i^{agg}}\\ &= k\cdot\varphi_i^{agg}\cdot\left[\left\langle\varphi_i^{gel}\cdot f(t) - \varphi^{void\_mortar}\cdot\left(\frac{(R_i+l_c)^3}{R_i^3}-1\right)\right\rangle^+\right]\end{aligned} \tag{9}$$

With $\varphi_i^{gel} = \varphi_{ref}^{gel}$ (Eq. (5)) since, for the first set of experiments, $AC = AC_{ref} = 8.1$ kg/m^3 and $\varphi_i^{agg} = \varphi_{tot}^{agg}$ (only one class of reactive particles).

In fact, in order to model the alkali consumption in a mixture, it is necessary to consider explicitly the decrease of the alkali content in the mortar due to the simultaneous consumption by all aggregates of

different sizes. This phenomenon is a problem of coupled diffusion, too hard to be considered in a simple "summary model". It is treated in detail in other works still in progress (and also in works such as Poyet et al. [6]).

Fig. 7 compares the ASR-expansion of mortars containing one size of reactive particles (M1 to M6) with the asymptotic expansion model (Section 4.1) and the time-dependent model developed in this section. It is observed that the time-dependent model represents the variation of the experimental data well, without any supplementary fitting of the parameters (except l_c and φ_{ref}^{gel} calculated from the first model).

Fig. 11 generalizes the calculations of the expansion for various alkali contents (AC) and aggregate sizes (R) for test durations of 50 and 500 days. It shows that, for a sufficient amount of alkali, the dependence of the expansion on the aggregate size can be seen as a pessimum effect. For these simulations, the expansion at 50 days is maximal for a reactive aggregate radius around 200–250 µm. This maximal expansion depends on the alkali content; it moves to 350 µm if alkali content is close to 6 kg/m^3. After longer times, the pessimum size increases (500–600 µm), since the alkali has had time to progress inside the aggregate.

Fig. 12 gives the expansion curves for test durations up to 500 days and several aggregate radii, the alkali content being 8.1 kg/m^3. This figure shows that expansion curves are stabilized only for aggregates having radii of less than around 300 µm.

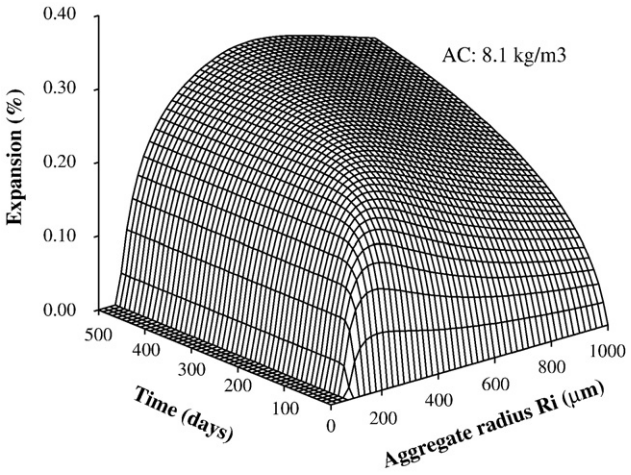

Fig. 12. Expansion curve simulations for different aggregate diameters, calculated using the time-dependent model (data: $k=1$, $l_c=11$ µm, $\varphi_{ref}^{gel}=0.066$, $\varphi^{void\_mortar}=0.17$, $AC=8.1$ kg/m^3, $AC_0=8.1$ kg/m^3, $AC_{th}=3.5$ kg/m^3, $R_{ref}=236$ µm, $t_{ref}=170$ days).

4.3. A synthesis of the part model and discussion

The asymptotic expansion and time dependent models summarize the main experimental observations given in the previous sections. They allow some important phenomena linked to the size of reactive aggregate to be interpreted easily. Firstly, the decrease of expansion for small aggregates is interpreted through the porous crown effect. Secondly, the slower expansion rate for large aggregates is explained using the alkali ingress kinetics.

It is interesting to note that the understanding of the pessimum effect of reactive aggregate size can be useful when fixing the parameters of accelerated laboratory tests. The model highlights the possibility of maximizing expansion, and consequently minimizing the test duration, by appropriate choices of both the alkali content and the aggregate size. This size must be sufficient to attenuate the connected porosity effect without making the duration of the test too long.

A direct application of this interpretation could be an original procedure aimed at minimizing the accelerated expansion test duration. For example, the authors are currently working on such a test clarification: it consists in extracting aggregates from an affected concrete, crushing them, and keeping only crushed particles of a given size. The mortars made with these aggregates (and an addition of alkalis) allow the potential for residual expansion of the concrete to be evaluated indirectly in the shortest possible time. Of course, this type of test must be combined with a particular model allowing the residual potential of the uncrushed aggregate in the concrete to be evaluated. Research is still in progress concerning this last topic.

5. Conclusion

This paper has presented the experimental measurements performed on 16 different mix-designs containing reactive siliceous limestone with special attention being paid to the proportions of

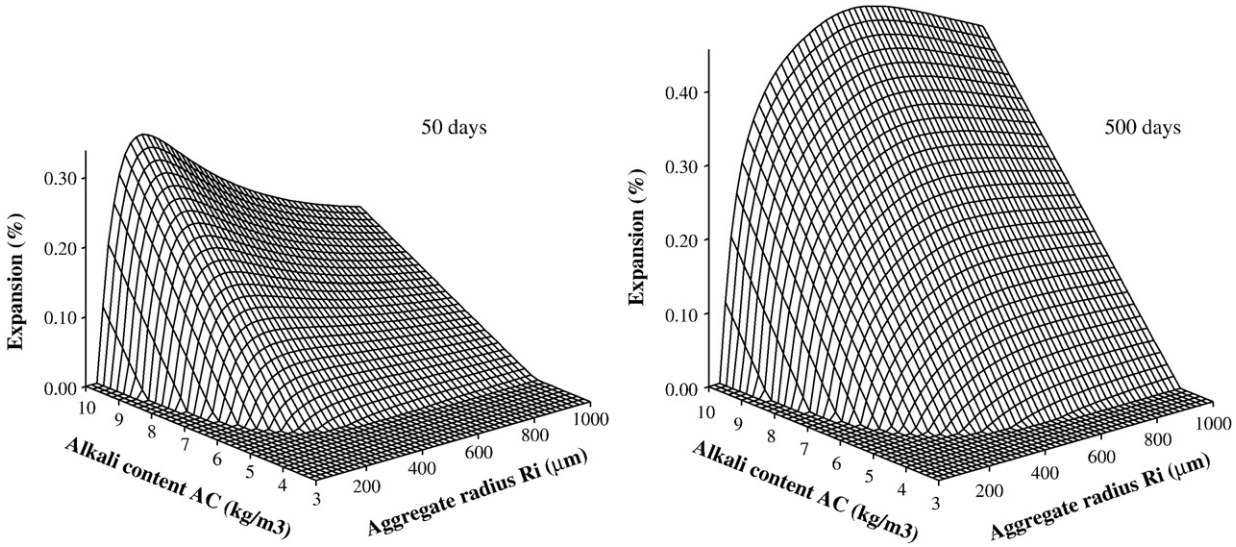

Fig. 11. Expansion versus alkali content (AC) and aggregate size (R) for test durations of 50 and 500 days, calculated using the time-dependent model (data: $k=1$, $l_c=11$ µm, $\varphi_{ref}^{gel}=0.066$, $\varphi^{void\_mortar}=0.17$, $AC_0=8.1$ kg/m^3, $AC_{th}=3.5$ kg/m^3, $R_{ref}=236$ µm, $t_{ref}=170$ days).

alkalis (Na_2O_{eq}) and reactive silica in the mixtures. It has been shown that:

- small reactive particles (under about 160 μm) do not cause expansion while coarse particles (0.63–1.25 mm) show the largest expansion (0.33%).
- ASR-expansion decreases with the amount of small particles when the mortars contain two sizes of aggregates (0–80 and 1250–3150 μm).

A first model shows that these results can be explained by the migration of ASR-gel in the porosity very close the reactive aggregate (less than 10 μm). The volume fraction of gel with respect to reactive aggregate has been considered as proportional to the alkali content of the mortar minus a threshold alkali content and to the proportion of reactive aggregates of each size compared to the content of all the reactive aggregates in the mortar. With these assumptions, the model predicts the expansions of the mortars containing two sizes of reactive aggregates.

In a second model, a time dependence of the expansion was introduced. It has been shown that, for a given duration of test and a given alkali content, the expansion is maximized for a specific range of aggregate size, which can be seen as a pessimum effect.

This approach allows a better understanding of the effects of aggregate size and alkali content on the expansion of mortars. It could also be useful for fixing the parameters of accelerated laboratory tests (maximizing expansion and minimizing duration of test). These tests and models will be used as a basis for the development of future models to assess the potential expansion of concrete containing alkali-reactive aggregates.

Notation

ε_{ASR}	expansion of mortar due to ASR
ε_i^{agg}	expansion of one reactive aggregate of class i
N_{rc}	number of classes of reactive aggregates
k	fraction of expansion due to ASR related to the expansion of reactive aggregates
l_c	distance of migration of the gel from the periphery of the aggregate
φ_i^{agg}	volume fraction of reactive aggregates of class i relative to the mortar
φ_{tot}^{agg}	volume fraction of reactive aggregates (total: all classes) relative to the mortar
φ_i^{gel}	volume fraction of gel related to the particles of class i ($\varphi_i^{gel} = V_i^{gel}/V_i^{agg}$)
φ_{ref}^{gel}	reference volume fraction of gel fitted from tests with AC_{ref}
φ^{void_mortar}	porosity of the mortar
V_i^{gel}	volume of ASR gel formed in only one reactive particle of class i
V_i^{poro}	volume of the porosity close to a reactive aggregate of class i, from which ASR gel can migrate without causing expansion
V_i^{agg}	volume of one reactive particle of class i
R_i	mean radius of reactive particle of class i
AC	alkali content of the mortar
AC_{th}	value of the threshold in alkali (taken equal to 3.5 kg/m^3),
AC_{ref}	alkali content of the mortar used to fit φ_{ref}^{gel} (8.1 kg/m^3),
$x(t)$	thickness of alkali penetration at a time t, from the paste to the center of the aggregate
R_{ref}	radius of the aggregate used in the mortar for which the reference time t_{ref} is fitted
t_{ref}	time necessary for alkali to reach the center of the aggregate of radius R_{ref}; fitted on experimental results such as $x(t_{ref}) = R_{ref}$
t	duration of test
$\varphi_i^{asr\_agg}(t)$	volume fraction of an aggregate of class i affected by ASR at time t

Acknowledgements

The authors are grateful to EDF for supporting this work.

References

[1] B. Capra, A. Sellier, Orthotropic modelling of alkali-aggregate reaction in concrete structures: numerical simulations, Mechanics of Materials 35 (8) (2003) 817–830.
[2] A. Sellier, E. Bourdarot, S. Multon, M. Cyr, E. Grimal, 2007, Assessment of the residual expansion for expertise of structures affected by AAR, 10th International Conference on Alkali-Aggregate Reaction, Broekmans M.A.T.M. and Wigum B.J. (Eds), Trondheim, Norway, 2008, pp.1004–1013.
[3] Y. Furusawa, H. Ohga, T. Uomoto, An analytical study concerning prediction of concrete expansion due to Alkali-Silica Reaction, 3rd CANMET/ACI International Conference on Durability of Concrete, Nice, France, 1994, pp. 757–779.
[4] A. Sellier, J.-P. Bournazel, A. Mébarki, Modelling the alkali aggregate reaction within a probabilistic frame-work, in: A. Shayan (Ed.), 10th International Conference on Alkali-Aggregate Reaction, Melbourne, Australia, 1996, pp. 694–701.
[5] Z.P. Bazant, A. Steffens, Mathematical model for kinetics of alkali silica reaction in concrete, Cement and Concrete Research 30 (3) (2000) 419–428.
[6] S. Poyet, A. Sellier, B. Capra, G. Foray, J.-M. Torrenti, H. Cognon, E. Bourdarot, Chemical modelling of Alkali Silica reaction: influence of the reactive aggregate size distribution, Materials and Structures 40 (2) (2007) 229–239.
[7] A. Suwito, W. Jin, Y. Xi, C. Meyer, A mathematical model for the pessimum effect of ASR in concrete, Concrete Science and Engineering 4 (13) (2002) 23–34.
[8] D. McConnell, R.C. Mielenz, W.Y. Holland, K.T. Greene, Cement-aggregate reaction in concrete, Journal of the American Concrete Institute, Proceedings 44 (2) (1947) 93–128.
[9] T.M. Kelly, L. Schuman, F.B. Hornibrook, A study of alkali-silica reactivity by means of mortar bar expansions, Journal of the American Concrete Institute, Proceedings 45 (1) (1948) 57–80.
[10] S. Diamond, N. Thaulow, A study of expansion due to alkali-silica reaction as conditioned by the grain size of the reactive aggregate, Cement and Concrete Research 4 (4) (1974) 591–607.
[11] D.W. Hobbs, W.A. Gutteridge, Particle size of aggregate and its influence upon the expansion caused by the alkali-silica reaction, Magazine of Concrete research 31 (109) (1979) 235–242.
[12] M. Kawamura, K. Takemoto, S. Hasaba, Application of quantitative EDXA analyses and microhardness measurements to the study of alkali-silica reaction mechanisms, in: G.M. Idorn, S. Rostam (Eds.), 6th International Conference of Alkalis in Concrete, 1983, pp. 167–174, Copenhague, Denmark.
[13] X. Zhang, G.W. Groves, The alkali-silica reaction in OPC/silica glass mortar with particular reference to pessimum effects, Advances in Cement Research 3 (9) (1990) 9–13.
[14] L. Hasni, Y. Gallias, M. Salomon, Appréciation des risques d'alcali- réaction dans les bétons de sable, Rapport de recherche n°41020, Centre Expérimental de Recherches et d'Etudes du Bâtiment et des Travaux Publics (CEBTP), St-Rémy-lès-Chevreuses, 1993, 53p.
[15] B.J. Wigum, W.J. French, Sequential examination of slowly expanding alkali-reactive aggregates in accelerated mortar bar testing, Magazine of Concrete research 48 (177) (1996) 281–292.
[16] C. Zhang, A. Wang, M. Tang, B. Wu, N. Zhang, Influence of aggregate size and aggregate size grading on ASR expansion, Cement and Concrete Research 29 (9) (1999) 1393–1396.
[17] T. Kuroda, S. Inoue, A. Yoshino, S. Nishibayashi, Effects of particle size, grading and content of reactive aggregate on ASR expansion of mortars subjected to autoclave method, in: M. Tang, M. Deng (Eds.), 12th International Conference on Alkali-Aggregate Reaction in Concrete, Beijing, China, 2004, pp. 736–743.
[18] K. Ramyar, A. Topal, O. Andic, Effects of aggregate size and angularity on alkali-silica reaction, Cement and Concrete Research 35 (11) (2005) 2165–2169.
[19] M. Moisson, M. Cyr, E. Ringot, A. Carles-Gibergues, Efficiency of reactive aggregate powder in controlling the expansion of concrete affected by alkali-silica reaction (ASR), in: M. Tang, M. Deng (Eds.), 12th International Conference on Alkali-Aggregate Reaction in Concrete, Beijing, China, 2004, pp. 617–624.
[20] AFPC-AFREM (Association Française Pour la Construction – Association Française de Recherche et Essais sur les Matériaux de construction), Durabilité des bétons. Méthodes recommandées pour la mesure des grandeurs associées à la durabilité. Mesure de la masse volumique apparente et de la porosité accessible à l'eau, Compte-Rendu des Journées Techniques, Toulouse, December 11–12 1997, pp. 121–124.
[21] T.N. Jones, A.B. Poole, Alkali-silica reaction in several U.K. concretes: the effect of temperature and humidity on expansion, and the significance of ettringite development, in: P.E. Grattan-Bellew (Ed.), 7th International Conference on Alkali-Aggregate Reaction in Concrete, Ottawa, Canada, 1986, pp. 446–450.
[22] P.K. Mukherjee, J.A. Bickley, Performance of glass as concrete aggregates, in: P.E. Grattan-Bellew (Ed.), 7th International Conference on Alkali-Aggregate Reaction in Concrete, Ottawa, Canada, 1986, pp. 36–42.
[23] A. Carles-Gibergues, M. Cyr, Interpretation of expansion curves of concrete subjected to accelerated alkali-aggregate reaction (AAR) tests, Cement and Concrete Research 32 (5) (2002) 691–700.
[24] K. Kodama, T. Nishino, Observation around the cracked region due to alkali-aggregate reaction by analytical electron microscope, in: P.E. Grattan-Bellew (Ed.), 7th International Conference on Alkali-Aggregate Reaction in Concrete, Ottawa, Canada, 1986, pp. 398–402.

[25] R.A. Kennerley, D.A. St John, L.H. Smith, A review of thirty years of investigation of the alkali-aggregate reaction in New Zealand, in: National Building Research Institute of the CSIR (Ed.), 5th International Conference on Alkali-Aggregate Reaction in Concrete, Cape Town, South Africa, 1981, S252/12, 9p.
[26] R.E. Oberholster, Alkali reactivity of siliceous rock aggregates: diagnosis of the reaction, testing of cement and aggregate and prescription of preventive measures, in: G.M. Idorn, S. Rostam (Eds.), 6th International Conference on Alkali-Aggregate Reaction in Concrete, Copenhagen, Denmark, 1983, pp. 419–433.
[27] D.W. Hobbs, Alkali-silica Reaction in Concrete, Thomas Telford, London, 1988.
[28] C.A. Rogers, R.D. Hooton, Reduction in mortar and concrete expansion with reactive aggregates due to alkali leaching, Cement, Concrete and Aggregates 13 (1) (1991) 42–49.
[29] M.D.A. Thomas, B.Q. Blackwell, P.J. Nixon, Estimating the alkali contribution from fly ash to expansion due to alkali-aggregate reaction in concrete, Magazine of Concrete Research 48 (177) (1996) 251–264.
[30] M.H. Shehata, M.D.A. Thomas, The effect of fly ash composition on the expansion of concrete due to alkali-silica reaction, Cement and Concrete Research 30 (7) (2000) 1063–1072.
[31] S. Multon, M. Cyr, A. Sellier, N. Leklou, L. Petit, Coupled effects of aggregate size and alkali content on ASR expansion, Cement and Concrete Research 38 (3) (2008) 350–359.
[32] J.S. Guédon-Dubied, G. Cadoret, V. Durieux, F. Martineau, P. Fasseu, V. van Overbecke, Study on Tournai limestone in Antoing Cimescaut Quarry, in: M.A. Bérubé, B. Fournier, B. Durand (Eds.), Petrological, chemical and alkali reactivity approach, 11th International Conference on Alkali-Aggregate Reaction in Concrete, Quebec City, Canada, 2000, pp. 335–344.